Nanoscale Research Letters
a SpringerOpen Journal

NANO EXPRESS Open Access

# Large-scale and controllable synthesis of metal-free nitrogen-doped carbon nanofibers and nanocoils over water-soluble $Na_2CO_3$

Qian Ding[1,2], Xueyin Song[1,2], Xiujuan Yao[1,2], Xiaosi Qi[1,2,3], Chak-Tong Au[4], Wei Zhong[1,2*] and Youwei Du[1,2]

**Abstract**

Using acetylene as carbon source, ammonia as nitrogen source, and $Na_2CO_3$ powder as catalyst, we synthesized nitrogen-doped carbon nanofibers (N-CNFs) and carbon nanocoils (N-CNCs) selectively at 450°C and 500°C, respectively. The water-soluble $Na_2CO_3$ is removed through simple washing with water and the nitrogen-doped carbon nanomaterials can be collected in high purity. The approach is simple, inexpensive, and environment-benign; it can be used for controlled production of N-CNFs or N-CNCs. We report the role of catalyst, the effect of pyrolysis temperature, and the photoluminescence properties of the as-harvested N-CNFs and N-CNCs.

**Keywords:** Carbon materials; Chemical vapor deposition; Water-soluble; Nitrogen-doped

## Background

Since Iijima's paper on helical carbon nanotubes, carbon nanomaterials (CNM) such as carbon nanotubes (CNT) and carbon nanofibers (CNF) have attracted great attention for their unique and outstanding electrical and mechanical properties [1-4]. The helical CNT are composed of five-membered or seven-membered rings, having carbon atoms of $sp^2$ and $sp^3$ hybridization [5,6]. It is envisaged that helical CNT exhibit novel and peculiar properties that are different from those of linear CNT. It has been suggested that CNM can be utilized in hydrogen storage [7,8], microwave absorption [9], and field emission [10,11]. Using CNM, scientists tried to fabricate nanosized electromagnetism devices [12-14] such as solenoid switch [15,16], miniature antenna [17,18], energy converter [19,20], and sensor [21,22].

For CNM generation, methods such as arc discharge, laser ablation, hydrothermal carbonization, solvothermal reduction, and chemical vapor deposition (CVD) are used [23-28]. Nonetheless, it is common to have metal impurities in the products, and the intrinsic properties of the as-obtained CNM are uncertain. The problem of metal impurities hinders further researches on CNM especially those related to electromagnetism features [29,30]. It is tedious and costly to remove metal impurities such as those of iron-group elements or their alloys [31]. Furthermore, unexpected defects or contaminants could be introduced into the CNM during purification procedures.

As a traditional method, CVD has its advantages [32,33]. By regulating parameters such as catalyst amount, reaction temperature, source flow rate, one can obtain different kinds of CNM. It is possible to control the CVD process for a designated outcome by adopting a particular set of reaction conditions [34,35]. Using acetylene as carbon precursor, Amelinckx et al. [36], Nitze et al. [37], and Tang et al. [38] obtained CNM with high purity and selectivity. Nevertheless, there are disadvantages such as high reaction temperature and outgrowth of desired product [28,39]. As for the growth mechanism of CNT in CVD processes, there are still controversies [40,41].

By doping foreign elements such as nitrogen and boron into the graphite lattices of CNM, Wang et al. [42], Ayala et al. [43], and Koós et al. [44] induced crystal and electronic changes to the structures of CNM [42-44]. It is noted that as support for palladium nanoparticles, helical CNM show excellent properties in electro-catalytic applications [45,46]. According to Franceschini et al. [47] and Mandumpal et al. [48], the introduction of nitrogen

* Correspondence: wzhong@nju.edu.cn
[1]Nanjing National Laboratory of Microstructures, Nanjing University, Nanjing 210093, People's Republic of China
[2]Jiangsu Provincial Laboratory for Nanotechnology, Nanjing University, Nanjing 210093, People's Republic of China
Full list of author information is available at the end of the article

restrains the aggregation of vacancies, resulting in defects and dislocations, as well as amplified curvature of graphite planes. The results of both experimental and theoretical studies demonstrate that compared to pure CNT, nitrogen-doped CNT show enhanced field emission properties and there is a shift of the dominant emission towards lower energies [49-51]. Through theoretical studies of heteroatom-substituted graphite systems, Hagiri et al. suggested that different heteroatom arrangements cause different spin-stable singlet and triplet states and that the substituted nitrogen atom as a spin cap induces the π electron excess [52]. When it comes to CNT utilization, high incorporation of nitrogen is desirable in promoting porosity and electrochemical reactivity of CNT. On the other hand, if CNT are supposed to be applied in semiconductor technology, low nitrogen-doping density is necessary.

Recently, we reported the large-scale synthesis of various kinds of non-doped CNM that are metal-free [53-55]. Herein, we report the use of $Na_2CO_3$ as catalyst for the selective formation of nitrogen-doped CNF (N-CNF) and nitrogen-doped CNC (N-CNC). We used $Na_2CO_3$ because it is water-soluble and can be removed from N-CNM through steps of water washing. We found that the $Na_2CO_3$ catalyst prepared by us is active and selective for mass formation of N-CNF and N-CNC. By means of CVD using $Na_2CO_3$ as catalyst, high-purity N-CNM can be obtained after washing the products with deionized water and ethanol. The approach is simple, inexpensive, and environment-benign, and can be used for mass production of high-purity N-CNF and N-CNC.

## Methods

All materials used were commercially available and analytically pure. In the present study, we employed $Na_2CO_3$ as catalyst. First, we mixed 10 g of $Na_2CO_3$ (in powder form) in 200 ml of deionized water at room temperature (RT) with continuous stirring. Once a transparent solution was obtained, the solution was kept at 80°C for several hours and allowed to cool down to RT for the precipitation of a white powder. The powder was filtered out, dried, and ground into tiny particles.

We placed 0.5 g of catalyst at the center of a ceramic boat with two open ends. The boat was then put inside a quartz tube with a thermocouple attached to its center. For the CVD reaction, we used acetylene as carbon source and ammonia as nitrogen source. After the reaction chamber was purged with argon for the elimination of oxygen, the sources were introduced into the system at either 450°C or 500°C at a $C_2H_2/NH_3$ flow rate ratio of 1:1 for 6 h. To study the effect of changing the flow rate ratio, we also introduced acetylene and ammonia at a $C_2H_2/NH_3$ flow rate ratio of 5:1 at 450°C for 6 h. After the reaction, argon was again introduced to protect the product from oxidation until the system was cooled down to RT. To remove the catalyst and to avoid organic outgrowth, the as-obtained products were repeatedly washed with deionized water and ethanol. Compared to the methods commonly used for CNM purification, the one used in the present study causes no damage to the desired product.

The morphologies of samples were examined using a transmission electron microscope (TEM) operated at an accelerating voltage of 200 kV and a field emission scanning electron microscope (FE-SEM) operated at an accelerating voltage of 5 kV. Fourier transform infrared (FTIR) spectroscopic studies of samples (in KBr pellets) were conducted over a Nocolet 510P spectrometer (Thermo Nocolet, Stanford, CT, USA). The surface analysis of products was carried out by means of X-ray photoelectron spectroscopy (XPS, PHI 5000 VersaProbe, UIVAC-PHI Inc., Chigasaki, Kanagawa, Japan). The products were examined on an X-ray powder diffractometer (XRD) at RT for phase identification using $CuK_\alpha$ radiation (model D/Max-RA, Rigaku Corporation, Tokyo, Japan). Raman spectroscopic investigations were performed over a Jobin-Yvon Labram HR800 instrument (Horiba, Ann Arbor, MI, USA) with 514.5-nm Ar laser excitation. The photoluminescence (PL) spectra were collected at RT over a spectrofluorophotometer (Shimadzu RF-5301 PC; Shimadzu Co. Ltd., Beijing, China) using a Xe lamp as light source. For PL investigation, about 0.1 mg of sample was ultrasonically dispersed in 5 ml of deionized water. Thermoanalysis was carried out using a thermal analysis system (NETZSCH STA 449C; NETZSCH Company, Shanghai, China) with the sample heated in air at a rate of 20°C/min.

## Results and discussion

We observed that when reaction temperature is higher than 500°C or lower than 400°C, the yield of CNM is small (TEM observation). Above 500°C, there is heavy decomposition of $Na_2CO_3$ into sodium oxide and $CO_2$, a situation unfavorable for CNM formation. Below 400°C, the decomposition of acetylene becomes unfavorable. Since there could be $Na_2CO_3$ decomposition at certain reaction temperatures, we do not choose weight change as a means to measure product yields. Shown in Table 1 are the conditions used for the generation of CNM.

Figure 1 shows the XRD patterns of the as-obtained and purified samples. The peaks of $Na_2CO_3$ can be indexed to the monoclinic phase of $Na_2CO_3$ (JCPDS 37–0451) with $a = 8.906$ Å, $b = 5.238$ Å, and $c = 6.045$ Å. Figure 1a,b is the patterns of C450 and C450N before and after purification, respectively. It is apparent that there are graphite carbon and $Na_2CO_3$ in CNM and N-CNM before purification. After repeated washing

**Table 1 Preparation summary of samples**

| Reaction temperature (°C) | Flow rate ratios ($C_2H_2/NH_3$) | Sample name |
|---|---|---|
| 450 | $C_2H_2$ only | C450 |
| 450 | 5:1 | C5N1 |
| 450 | 1:1 | C450N |
| 500 | 1:1 | C500N |

with water and ethanol, there is complete elimination of $Na_2CO_3$ as well as ethanol-soluble organic outgrowth. With the incorporation of nitrogen, there is decline of graphite signal intensity.

Figure 2 shows the FE-SEM and TEM images of the purified samples. The selectivity to carbon species was determined statistically according to the number of counts of CNM at different regions of the TEM and FE-SEM images. The images of C5N1 are not given here for they are similar to those of C450 and C450N. As shown in Figure 2a,d, the major constitution of C450 is long and composed of linear carbon nanofibers (LCNF). The rest is irregular carbon complexes, and there is no detection of helical carbon nanofibers (HCNF). According to the TEM images, the average diameter of LCNF is *ca*. 20 nm. In other words, LCNF can be synthesized in large scale with high selectivity using this method. As shown in Figure 2b,e, the major product of C450N is still LCNF, but there is sighting of helical structures. As shown in the inset of Figure 2b, there are sightings of long HCNF. The TEM images indicate that the obtained LCNF and HCNF have average diameter of *ca*. 30 nm. The results show that with the doping of nitrogen into graphitic lattices, there is change in CNM morphology: the generation of helical structures. When the reaction temperature is 500°C, the major product of C500N is the long spiny carbon nanofibers (SCNF) (Figure 2c,f), having average diameter of *ca*. 100 nm. It is known that reaction temperature is a parameter that affects the synthesis of nanomaterials in terms of morphology, structure, and component. Through the control of morphology, structure, and/or component, it is possible to obtain CNM of particular properties. In the case of long SCNF, the material is enriched with multi-pillar structures and is relatively large in specific surface area. With such physical properties, the material can be used as support for better dispersion of nanoparticles.

XPS O1*s*, C1*s*, and N1*s* spectra were obtained for the determination of surface composition and bonding environment of C and N atoms of the purified samples. The nitrogen content of a particular product is defined as 100 N/(C + N + O) at.%. As depicted in Table 2, the amounts of nitrogen in C450, C5N1, C450N, and C500N are 0%, 1.77%, 2.86%, and 2.10%, respectively. It is noted that the oxygen contents of the four samples are about 4%. Based on the results, we deduce that a rise of nitrogen source at reaction temperature of 450°C results in products higher in nitrogen content. However, with a rise of reaction temperature from 450°C to 500°C, there is a slight decline of nitrogen content. It is plausible that $NH_3$ decomposition is enhanced with temperature rise, but the concurrent decomposition of catalyst goes against the formation of nitrogen-doped CNT. That C500N is lower than C450N in nitrogen content is a net consequence of the two actions.

According to some researches, the electronic properties of CNM can be tuned by doping nitrogen atoms into the carbon lattices and be regulated by controlling the type, concentration, and content of dopants [56,57]. We observe that C450, C5N1, C450N, and C500N show C1*s*, N1*s*, and O1*s* peaks at around 284, 400, and 532 eV, respectively (Figure 3a). As shown in Figure 3b, the C1*s* peak can be deconvoluted into two components at 284.1 and 285.8 eV. The stronger one at 284.1 eV is ascribed to the carbon of $sp^2$-hybridized C-C bonds

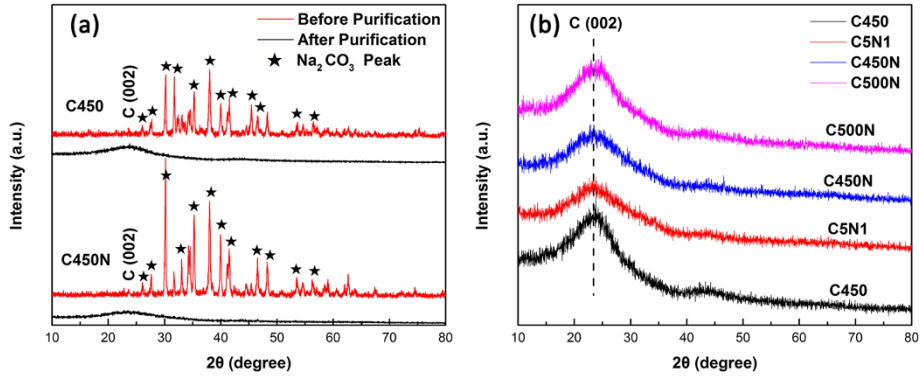


**Figure 1** XRD patterns of (a) as-obtained and (b) purified samples.

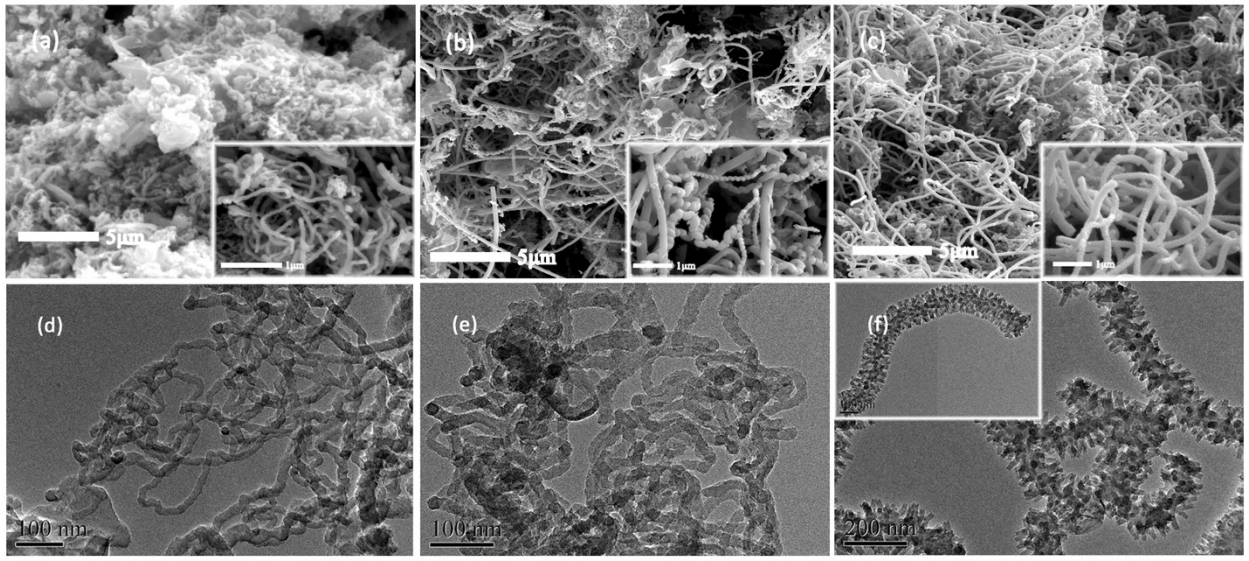


**Figure 2 FE-SEM and TEM images of C450, C450N, and C500N.** FE-SEM images of **(a)** C450, **(b)** C450N, and **(c)** C500N, and the TEM images of **(d)** C450, **(e)** C450N, and **(f)** C500N (insets are the corresponding high-magnification images).

whereas that at 285.8 eV to carbon of C-N bonds. There are three primary statuses of nitrogen configuration in nitrogen-doped CNMs: graphitic (substitutional nitrogen), pyridine-like, and pyrrole-like. In order to analyze the electronic state of nitrogen atoms in CNMs, we focused our attention especially to the N1*s* spectra, as revealed in Figure 3c. The peak around 398.3 eV is attributed to $sp^3$-hybridized nitrogen of the tetrahedral phase; the nitrogen is pyridine-type and is connected with the defective graphite sheets. The peak at 399.8 eV is ascribable to nitrogen with a local structure alike that of pyrrole, and the nitrogen is hence considered as pyrrole-type. The peak at 401.0 eV corresponds to $sp^2$-hybridized nitrogen of trigonal phase, and the nitrogen is graphite-type or substitutional type. The composition of the three types of nitrogen is reflected by the area ratio of the corresponding N1*s* peaks. With rise of reaction temperature from 400°C to 500°C, there is a significant increase of graphitic nitrogen relative to that of pyridine-type nitrogen. It is deduced that the formation of graphitic configuration becomes more favorable with the rise of temperature.

Figure 4 shows the Raman spectra of C450, C5N1, C450N, and C500N. Each of the samples exhibits two peaks. The one at about 1,340 $cm^{-1}$ (called D band) is associated with amorphous carbon relating to the vibration of carbon atoms with dangling bonds of disordered graphite. The peak at about 1,600 $cm^{-1}$ (called G band) is related to the double-degenerate E2*g* mode of graphite, corresponding to the vibration of triple-degenerate $sp^2$ hybrid bond. The intensity ratio of G band and D band ($I_G/I_D$) is generally used to identify the crystallinity of graphite. Lower $I_G/I_D$ means more defect or vacancy. The intensity ratios of C450, C5N1, C450N, and C500N are listed in Table 3.

**Table 2 Nitrogen content of samples**

| Sample name | Nitrogen content (at.%) |
|---|---|
| C450 | 0 |
| C5N1 | 1.77 |
| C450N | 2.86 |
| C500N | 2.10 |

Compared with C5N1, C450N is lower in $I_G/I_D$ value. The $C_2H_2/NH_3$ flow rate ratio for the formation of C5N1 is 5:1 whereas that of C450N is 1:1. In other words, with a source flow richer in nitrogen, there is rise of nitrogen content, and with more defects or vacancies in N-CNM, there is decline of $I_G/I_D$ value. With the rise of reaction temperature from 450°C to 500°C, there is slight decrease of nitrogen content but enhanced formation of amorphous carbon, and the net result is the further decline of $I_G/I_D$ value.

The PL spectra of C450, C5N1, and C450N obtained with an excitation source of 220 nm wavelength are showed in Figure 5a. It is known that pristine CNM exhibits strong UV PL at 368 nm at RT. In the present study, we find that by doping of nitrogen into CNM, there is enhancement of UV PL, and PL signal intensifies with the rise of nitrogen content. The peak at 468 nm is a sideband peak, and its intensity is usually weaker than that of 368 nm. The super peak at about 440 nm is the double wavelength of 220 nm attributable to the excitation wavelength. In Figure 5b, with the excitation

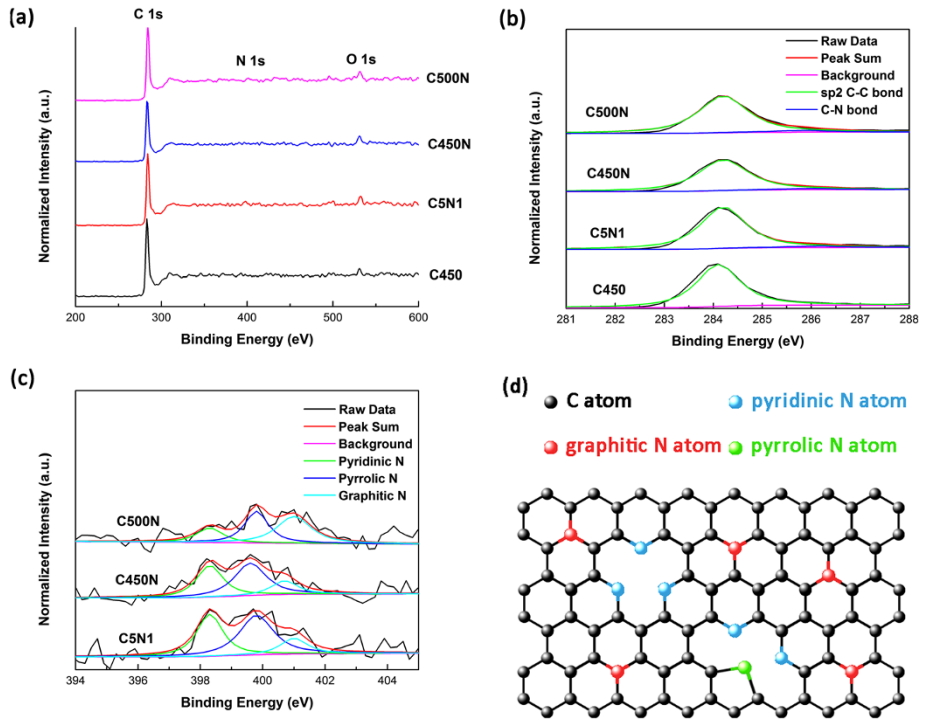


**Figure 3 XPS spectra of the purified samples. (a)** Survey scan, **(b)** C1*s* spectra, **(c)** N1*s* spectra, and **(d)** illustration of nitrogen configuration.

wavelength increasing from 220 to 280 nm, the intensity of the PL peak at 368 nm decreases. When the excitation wavelength reaches 300 nm, there is the detection of a peak at about 410 nm over the C450N sample as shown in Figure 5c. The peak is a purple band. There is no detection of such a peak at about 410 nm over the C450 and C5N1 samples. We ascribe the phenomenon to the impurity transition level induced by doping nitrogen of a certain concentration into the graphite lattice. It is hence possible to modulate the luminescence peak in a controllable manner from visible light to the UV band by doping CNT with different concentrations of nitrogen.

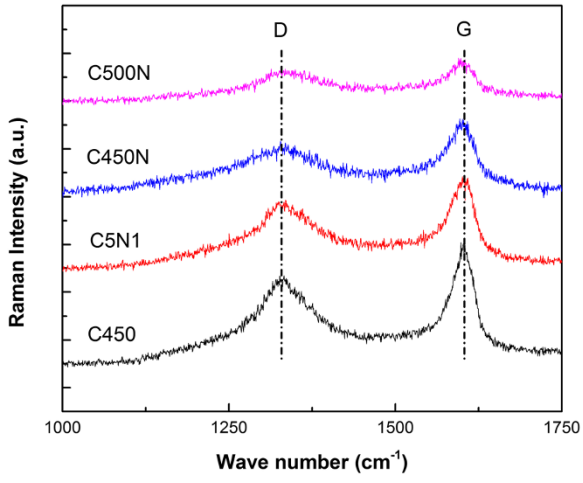


**Figure 4 Raman spectra of C450, C5N1, C450N, and C500N.**

Figure 6 is the FTIR spectrum of C450N. The peak at 3,455.8 $cm^{-1}$ can be ascribed to the stretching vibration of unsaturated –CH = CH–. The peaks at 1,610.3 and 1,441.9 $cm^{-1}$ are ascribed to –C-H stretching vibration while that at 879.4 $cm^{-1}$ to –C-H deformation vibration. Compared to the FTIR result of our previous study [53], the nitrogen-doped CNM shows weaker peak intensity and poorer transmittance plausibly due to the presence of defects or vacancies.

We tested the oxidation resistance of C450 and C450N. As shown in Figure 7, both samples are sharply oxidized at about 460°C, at a temperature lower than that for the oxidation of CNM generated in CVD processes using iron-group metals or their alloys as catalysts [58,59]. Furthermore, the oxidation of C450N starts at about 460°C, and it is not so with C450. The results suggest that there are more active

**Table 3 The $I_G/I_D$ intensity ratios of all samples**

| Sample name | $I_G/I_D$ |
|---|---|
| C450 | 1.326 |
| C5N1 | 1.287 |
| C450N | 1.255 |
| C500N | 1.239 |

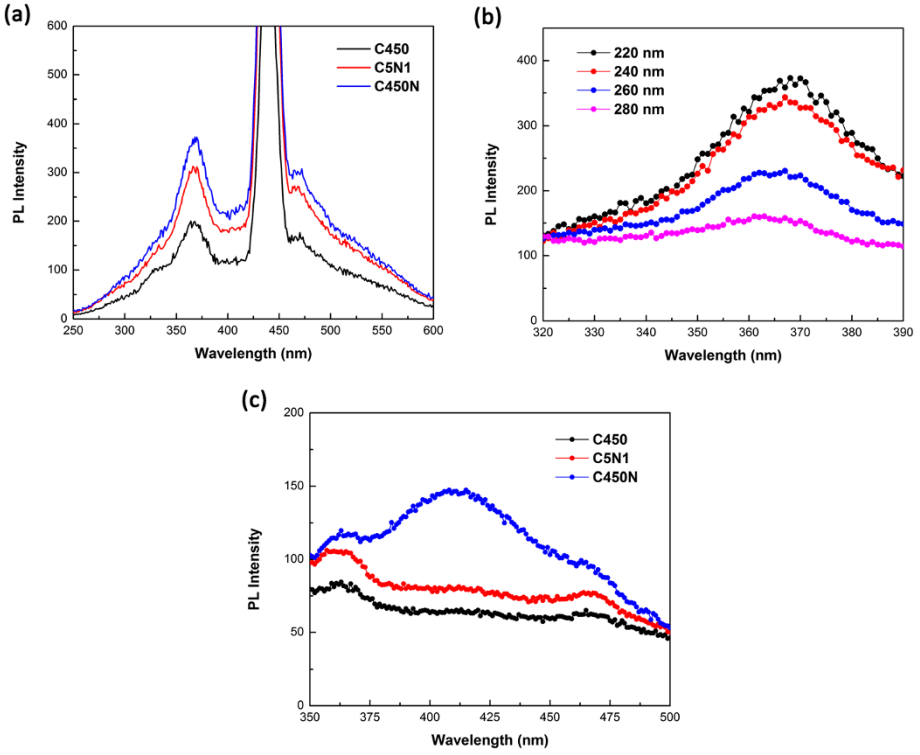


**Figure 5 PL spectra of C450, C5N1, and C450. (a)** C450, C5N1, and C450 with an excitation wavelength of 220 nm. **(b)** C450N with different excitation wavelengths ranging from 220 to 280 nm. **(c)** C450, C5N1, and C450 with an excitation wavelength of 300 nm.

defects and amorphous carbon in C450N in comparison with C450.

## Conclusions

By controlling the acetylene decomposition temperature, N-CNF and N-CNC can be selectively synthesized in large scale over $Na_2CO_3$. Due to the water-soluble property of $NaCO_3$, the products can be obtained in high purity through steps of water and ethanol washing. The CVD process using $Na_2CO_3$ as catalyst is simple, inexpensive, and environment-benign. We detect graphitic, pyridine-like as well as pyrrole-like N species in the nitrogen-doped CNM. Compared to the non-doped pristine CNM, the nitrogen-doped ones show enhanced UV PL intensity.

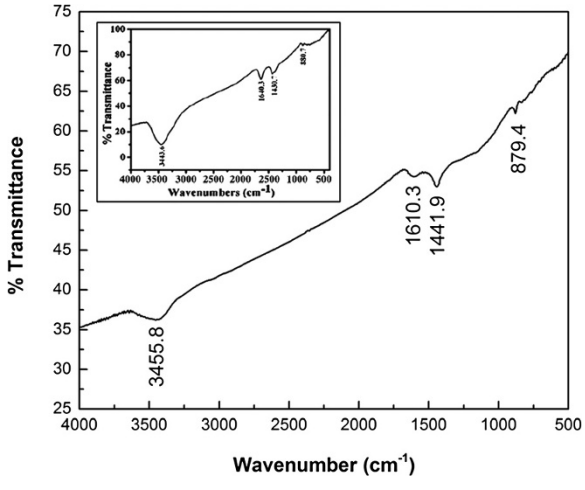


**Figure 6 FTIR spectrum of C450N.** Inset is the FTIR spectrum of C450, after [53].

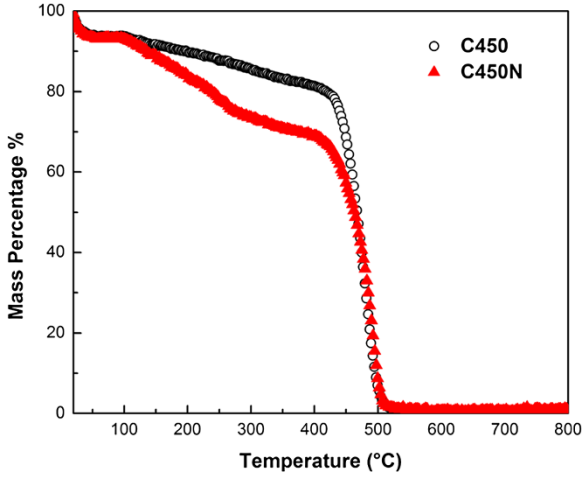


**Figure 7 TGA curve of C450 and C450N.**

**Competing interests**
The authors declare that they have no competing interests.

**Authors' contributions**
WZ and QD designed the study and guided this work. XYS, XJY, and XSQ participated in the design of the study. QD carried out the experiments, analyzed the data, and drafted the manuscript. WZ and CTA checked and revised the manuscript. CTA and YWD gave precious suggestions to this work. All authors read and approved the final manuscript.

**Acknowledgements**
This work was supported by the National Natural Science Foundation of China (grant no. 11174132), the National Key Project for Basic Research (grant nos. 2010CB923402 and 2011CB922102), and PAPD, People's Republic of China.

**Author details**
[1]Nanjing National Laboratory of Microstructures, Nanjing University, Nanjing 210093, People's Republic of China. [2]Jiangsu Provincial Laboratory for Nanotechnology, Nanjing University, Nanjing 210093, People's Republic of China. [3]College of Science, Guizhou University, Guiyang 550025, People's Republic of China. [4]Chemistry Department, Hong Kong Baptist University, Hong Kong 852, People's Republic of China.

Received: 11 July 2013 Accepted: 17 December 2013
Published: 27 December 2013

**References**

1. Iijima S: **Helical microtubules of graphitic carbon.** *Nature* 1991, **354:**56–58.
2. Iijima S, Ichihashi T: **Single-shell carbon nanotubes of 1-nm diameter.** *Nature* 1993, **363:**603–605.
3. Bethune DS, Johnson RD, Salem JR, Devries MS, Yannoni CS: **Atoms in carbon cages - the structure and properties of endohedral fullerenes.** *Nature* 1993, **366:**123–128.
4. Rodriguez NM, Chambers A, Baker RTK: **Catalytic engineering of carbon nanostructures.** *Langmuir* 1995, **11:**3862–3866.
5. Tamura R, Tsukada M: **Electronic states of the cap structure in the carbon nanotube.** *Phys Rev B* 1995, **52:**6015–6026.
6. Terrones H, Terrones M, Hernandez E, Grobert N, Charlier JC, Ajayan PM: **New metallic allotropes of planar and tubular carbon.** *Phys Rev Lett* 2000, **84:**1716–1719.
7. Tans SJ, Verschueren ARM, Dekker C: **Room-temperature transistor based on a single carbon nanotube.** *Nature* 1998, **393:**49–52.
8. Bai XD, Zhong DY, Zhang GY, Ma XC, Liu S, Wang EG, Chen Y, Shaw DT: **Hydrogen storage in carbon nitride nanobells.** *Appl Phys Lett* 2001, **79:**1552–1554.
9. Wadhawan A, Garrett D, Perez JM: **Nanoparticle-assisted microwave absorption by single-wall carbon nanotubes.** *Appl Phys Lett* 2003, **83:**2683–2685.
10. Adessi C, Devel M: **Theoretical study of field emission by single-wall carbon nanotubes.** *Phys Rev B* 2000, **62:**13314–13317.
11. Shim M, Javey A, Kam NWS, Dai HJ: **Polymer functionalization for air-stable n-type carbon nanotube field-effect transistors.** *J Am Chem Soc* 2001, **123:**11512–11513.
12. Dai HJ, Hafner JH, Rinzler AG, Colbert DT, Smalley RE: **Nanotubes as nanoprobes in scanning probe microscopy.** *Nature* 1996, **384:**147–150.
13. Tsukagoshi K, Alphenaar BW, Ago H: **Coherent transport of electron spin in a ferromagnetically contacted carbon nanotube.** *Nature* 1999, **401:**572–574.
14. Yang CK, Zhao J, Lu JP: **Magnetism of transition-metal/carbon-nanotube hybrid structures.** *Phys Rev Lett* 2003, **90:**257203.
15. Liu L, Jayanthi CS, Tang MJ, Wu SY, Tombler TW, Zhou CW, Alexseyev L, Kong J, Dai H: **Controllable reversibility of an sp(2) to sp(3) transition of a single wall nanotube under the manipulation of an AFM tip: a nanoscale electromechanical switch?** *Phys Rev Lett* 2000, **84:**4950–4953.
16. Banerjee P, Wolny F, Pelekhov DV, Herman MR, Fong KC, Weissker U, Muhl T, Obukhov Y, Leonhardt A, Buchner B, Hammel PC: **Magnetization reversal in an individual 25 nm iron-filled carbon nanotube.** *Appl Phys Lett* 2010, **96:**252505–252505. -3.
17. Dresselhaus MS: **Applied physics - nanotube antennas.** *Nature* 2004, **432:**959–960.
18. Kempa K, Rybczynski J, Huang ZP, Gregorczyk K, Vidan A, Kimball B, Carlson J, Benham G, Wang Y, Herczynski A, Ren ZF: **Carbon nanotubes as optical antennae.** *Adv Mater* 2007, **19:**421.
19. Zhang J, Hu YS, Tessonnier JP, Weinberg G, Maier J, Schlogl R, Sheng DS: **CNFs@CNTs: superior carbon for electrochemical energy storage.** *Adv Mater* 2008, **20:**1450.
20. Guldi DM, Sgobba V: **Carbon nanostructures for solar energy conversion schemes.** *Chem Commun* 2011, **47:**606–610.
21. Baughman RH, Zakhidov AA, de Heer WA: **Carbon nanotubes - the route toward applications.** *Science* 2002, **297:**787–792.
22. Kong J, Franklin NR, Zhou CW, Chapline MG, Peng S, Cho KJ, Dai H: **Nanotube molecular wires as chemical sensors.** *Science* 2000, **287:**622–625.
23. Loiseau A, Willaime F, Demoncy N, Hug G, Pascard H: **Boron nitride nanotubes with reduced numbers of layers synthesized by arc discharge.** *Phys Rev Lett* 1996, **76:**4737–4740.
24. Journet C, Maser WK, Bernier P, Loiseau A, delaChapelle ML, Lefrant S, Deniard P, Lee R, Fischer JE: **Large-scale production of single-walled carbon nanotubes by the electric-arc technique.** *Nature* 1997, **388:**756–758.
25. Liu ZP, Zhou XF, Qian YT: **Synthetic methodologies for carbon nanomaterials.** *Adv Mater* 2010, **22:**1963–1966.
26. Sawant SY, Somani RS, Bajaj HC: **A solvothermal-reduction method for the production of horn shaped multi-wall carbon nanotubes.** *Carbon* 2010, **48:**668–672.
27. Ebbesen TW, Ajayan PM: **Large-scale synthesis of carbon nanotubes.** *Nature* 1992, **358:**220–222.
28. Cassell AM, Raymakers JA, Kong J, Dai HJ: **Large scale CVD synthesis of single-walled carbon nanotubes.** *J Phys Chem B* 1999, **103:**6484–6492.
29. Banks CE, Crossley A, Salter C, Wilkins SJ, Compton RG: **Carbon nanotubes contain metal impurities which are responsible for the "electrocatalysis" seen at some nanotube-modified electrodes.** *Angew Chemie-Int Ed* 2006, **45:**2533–2537.
30. Jones CP, Jurkschat K, Crossley A, Compton RG, Riehl BL, Banks CE: **Use of high-purity metal-catalyst-free multiwalled carbon nanotubes to avoid potential experimental misinterpretations.** *Langmuir* 2007, **23:**9501–9504.
31. Park TJ, Banerjee S, Hemraj-Benny T, Wong SS: **Purification strategies and purity visualization techniques for single-walled carbon nanotubes.** *J Mater Chem* 2006, **16:**141–154.
32. Leal MCA, Horna CD: **CVD and the new technologies.** *An Quim* 1991, **87:**445–456.
33. Li QW, Yan H, Cheng Y, Zhang J, Liu ZF: **A scalable CVD synthesis of high-purity single-walled carbon nanotubes with porous MgO as support material.** *J Mater Chem* 2002, **12:**1179–1183.
34. Kong J, Zhou C, Morpurgo A, Soh HT, Quate CF, Marcus C, Dai H: **Synthesis, integration, and electrical properties of individual single-walled carbon nanotubes.** *Appl Phys A Mater Sci Process* 1999, **69:**305–308.
35. Su M, Zheng B, Liu J: **A scalable CVD method for the synthesis of single-walled carbon nanotubes with high catalyst productivity.** *Chem Phys Lett* 2000, **322:**321–326.
36. Amelinckx S, Zhang XB, Bernaerts D, Zhang XF, Ivanov V, Nagy JB: **A formation mechanism for catalytically grown helix-shaped graphite nanotubes.** *Science* 1994, **265:**635–639.
37. Nitze F, Abou-Hamad E, Wagberg T: **Carbon nanotubes and helical carbon nanofibers grown by chemical vapour deposition on C60 fullerene supported Pd nanoparticles.** *Carbon* 2010, **49:**1101–1109.
38. Tang NJ, Wen JF, Zhang Y, Liu FX, Lin KJ, Du YW: **Helical carbon nanotubes: catalytic particle size-dependent growth and magnetic properties.** *ACS NANO* 2010, **4:**241–250.
39. Li YY, Sakoda A: **Growth of carbon nanotubes and vapor-grown carbon fibers using chemical vapor deposition of methane.** *J Chin Inst Chem Eng* 2002, **33:**483–489.
40. Lee CJ, Lyu SC, Cho YR, Lee JH, Cho KI: **Diameter-controlled growth of carbon nanotubes using thermal chemical vapor deposition.** *Chem Phys Lett* 2001, **341:**245–249.
41. Emmenegger C, Bonard JM, Mauron P, Sudan P, Lepora A, Grobety B, Züttela A, Schlapbach L: **Synthesis of carbon nanotubes over Fe catalyst on aluminium and suggested growth mechanism.** *Carbon* 2003, **41:**539–547.
42. Wang B, Ma YF, Wu YP, Li N, Huang Y, Chen YS: **Direct and large scale electric arc discharge synthesis of boron and nitrogen doped single-**

walled carbon nanotubes and their electronic properties. *Carbon* 2009, **47:**2112–2115.
43. Ayala P, Arenal R, Rummeli M, Rubio A, Pichler T: **The doping of carbon nanotubes with nitrogen and their potential applications.** *Carbon* 2010, **48:**575–586.
44. Koós AA, Dillon F, Obraztsova EA, Crossley A, Grobert N: **Comparison of structural changes in nitrogen and boron-doped multi-walled carbon nanotubes.** *Carbon* 2010, **48:**3033–3041.
45. Hu GZ, Nitze F, Sharifi T, Barzegar HR, Wagberg T: **Self-assembled palladium nanocrystals on helical carbon nanofibers as enhanced electrocatalysts for electro-oxidation of small molecules.** *J Mater Chem* 2012, **22:**8541–8548.
46. Hu GZ, Nitze F, Barzegar HR, Sharifi T, Mikolajczuk A, Tai CW, Borodzinski A, Wågberg T: **Palladium nanocrystals supported on helical carbon nanofibers for highly efficient electro-oxidation of formic acid, methanol and ethanol in alkaline electrolytes.** *J Power Sources* 2012, **209:**236–242.
47. Franceschini DF, Achete CA, Freire FL: **Internal-stress reduction by nitrogen incorporation in hard amorphous-carbon thin-films.** *Appl Phys Lett* 1992, **60:**3229–3231.
48. Mandumpal J, Gemming S, Seifert G: **Curvature effects of nitrogen on graphitic sheets: structures and energetics.** *Chem Phys Lett* 2007, **447:**115–120.
49. Wang XB, Liu LQ, Zhu DB, Zhang L, Ma HZ, Yao N, Zhang B: **Controllable growth, structure, and low field emission of well-aligned $CN_x$ nanotubes.** *J Phys Chem B* 2002, **106:**2186–2190.
50. Wang C, Qiao L, Qu CQ, Zheng WT, Jiang Q: **First-principles calculations on the emission properties of pristine and N-doped carbon nanotubes.** *J Phys Chem C* 2009, **113:**812–818.
51. Li LJ, Glerup M, Khlobystov AN, Wiltshire JG, Sauvajol JL, Tavlor RA, Nicholas RJ: **The effects of nitrogen and boron doping on the optical emission and diameters of single-walled carbon nanotubes.** *Carbon* 2006, **44:**2752–2757.
52. Hagiri I, Takahashi N, Takeda K: **Theoretical possibility of the variety of ground-state spin arrangements created by the spin hole and spin cap in a pi-conjugated system.** *J Phys Chem A* 2004, **108:**2290–2304.
53. Qi XS, Ding Q, Zhang H, Zhong W, Au C, Du YW: **Large-scale and controllable synthesis of metal-free carbon nanofibers and carbon nanotubes over water-soluble $Na_2CO_3$.** *Mater Lett* 2012, **81:**135–137.
54. Qi XS, Zhong W, Yao XJ, Zhang H, Ding Q, Wu Q, Deng Y, Au C, Du Y: **Controllable and large-scale synthesis of metal-free carbon nanofibers and carbon nanocoils over water-soluble NaxKy, catalysts.** *Carbon* 2012, **50:**646–658.
55. Qi X, Ding Q, Zhong W, Au C-T, Du Y: **Controllable synthesis and purification of carbon nanofibers and nanocoils over water-soluble $NaNO_3$.** *Carbon* 2013, **56:**383–385.
56. Glerup M, Castignolles M, Holzinger M, Hug G, Loiseau A, Bernier P: **Synthesis of highly nitrogen-doped multi-walled carbon nanotubes.** *Chem Commun* 2003, **2003:**2542–2543.
57. He MS, Zhou S, Zhang J, Liu ZF, Robinson C: **CVD growth of N-doped carbon nanotubes on silicon substrates and its mechanism.** *J Phys Chem B* 2005, **109:**9275–9279.
58. Murakami Y, Miyauchi Y, Chiashi S, Maruyama S: **Characterization of single-walled carbon nanotubes catalytically synthesized from alcohol.** *Chem Phys Lett* 2003, **374:**53–58.
59. Chen CM, Dai YM, Huang JG, Jehng JM: **Intermetallic catalyst for carbon nanotubes (CNTs) growth by thermal chemical vapor deposition method.** *Carbon* 2006, **44:**1808–1820.

doi:10.1186/1556-276X-8-545
**Cite this article as:** Ding *et al.*: Large-scale and controllable synthesis of metal-free nitrogen-doped carbon nanofibers and nanocoils over water-soluble $Na_2CO_3$. *Nanoscale Research Letters* 2013 **8**:545.